

Experimental Assessment of Environmental and Economic Impacts of Dampers' and Filters' Faults in a Typical Air-Handling Unit in Southern Italy



Antonio Rosato^{ID}, Rita Mercuri^{*ID}, Francesco Romanucci^{ID}, Mohammad El Youssef^{ID}

Department of Architecture and Industrial Design, University of Campania Luigi Vanvitelli, Aversa 81031, Italy

Corresponding Author Email: rita.mercuri@unicampania.it

Copyright: ©2024 The authors. This article is published by IIETA and is licensed under the CC BY 4.0 license (<http://creativecommons.org/licenses/by/4.0/>).

<https://doi.org/10.18280/ijcmem.120404>

ABSTRACT

Received: 26 May 2024

Revised: 25 November 2024

Accepted: 11 December 2024

Available online: 27 December 2024

Keywords:

air-handling unit, damper fault, filter fault, carbon dioxide emissions, operating costs, fault detection and diagnosis

Heating, Ventilation and Air-Conditioning (HVAC) systems are responsible of 50-60% of energy demand of the building sector. The scientific literature highlights that HVAC units are frequently operated under faulty conditions that can significantly affect their performance. In this paper, the performance of a typical single-duct dual-fan constant air volume Air-Handling Unit (AHU) is investigated through a number of experiments performed during Italian cooling and heating seasons under both fault free and faulty scenarios. The AHU operation is analysed while artificially introducing seven typical faults: return air damper kept always closed; fresh air damper kept always closed; fresh air damper kept always open; exhaust air damper kept always closed; supply air filter clogged at 50%; fresh air filter clogged at 50%; return air filter clogged at 50%. The faulty and fault free tests are compared to assess the environmental and economic performance impacts. The experimental data highlighted that the most adverse fault is that one corresponding to the exhaust air dumper kept always closed; in particular, it increases both the daily global equivalent CO₂ emissions and the daily operating costs up to 110% in comparison with the fault free conditions.

1. INTRODUCTION

About 36% of the world's energy demand and 37% of greenhouse gas emissions are attributed to buildings. Heating, Ventilation and Air-Conditioning (HVAC) systems play a major role, accounting for between 50 and 60% of building energy demand and between 10 and 20% of overall energy consumption [1, 2]. The scientific literature points out that HVAC systems are frequently operated under faulty conditions due to lack of proper maintenance, components' failure or incorrect installation, significantly affecting their energy, environmental and economic performance [3, 4]. Companies typically use two different types of maintenances (reactive or preventive maintenance) to ensure the reliability of HVAC units [5, 6]. The Automated Fault Detection and Diagnosis (AFDD), which automatically detects and diagnoses deviations from normal operation problems, could address some critical points that both approaches have [2, 7, 8]. According to several studies [6, 8, 9], AFDD tools can provide a number of advantages, including enhancing indoor comfort and equipment lifespans, as well as reducing greenhouse gas emissions, energy costs, maintenance and operating expenses [10, 11]. The techniques used for conducting AFDD analyses can be categorized into: (i) quantitative model-based, (ii) qualitative model-based, and (iii) data-driven methods [7, 9, 12]. The data-driven methods are gaining more and more interest mainly thanks to those facts the (i) they can enhance the accuracy of detection and

diagnosis, as well as (ii) they can be adopted even when there's limited physics-based knowledge [7, 8, 13]. However, data driven-based AFDD tools can be exploited to identify faults by analyzing changes in specific variable patterns and looking for causes based on the comparison between normal and faulty field operation. [7, 8, 13]. Therefore, they necessitate labelled, dependable, cost-effective, and scalable experimental data; however, acquiring such data is really challenging and time-consuming [7, 8, 14]. It's worth noting that only a limited number of studies performed quantitative analyses by using real-world data assessing how different types and severities of faults can impact users' comfort, key parameter patterns, energy usage, greenhouse gas emissions, operational and maintenance expenses, and equipment lifespan [4, 15-17]. Only few studies have been focused on single-duct dual-fan constant air volume air-handling units (AHUs) [17-19]. Even if the occurrence of dampers' faults in AHUs has been analysed in a number of scientific works [20], faults on filters of AHUs have been studied only in very few papers [20]; in particular, none of them has been carried out with reference to Italian climatic conditions. In light of these observations, further efforts could be crucial in shaping the future advancement of AFDD technologies with reference to the occurrence of faults on dampers and filters in AHUs. In this study, the operation of a typical single-duct dual-fan constant air volume AHU, integrated in the SENS i-Lab of the Department of Architecture and Industrial Design of the University of Campania Luigi Vanvitelli (located in Aversa,

south of Italy), has been experimentally characterized on the basis of daily tests performed under both normal and faulty conditions during both Italian summer and winter seasons. In particular, the operation of the AHU has been analysed while artificially introducing the following 7 different typical faults: (1) return air damper kept always closed (stuck at 0%), (2) fresh air damper kept always closed (stuck at 0%), (3) fresh air damper kept always open (stuck at 100%), (4) exhaust air damper kept always closed (stuck at 0%), (5) fresh air filter partially clogged at 50%, (6) supply air filter partially clogged at 50% and (7) return air filter partially clogged at 50%. The experimental data have been investigated comparing the ones obtained under faulty conditions with data acquired under fault-free operation under similar boundary conditions. The aim of this investigation is to assess the impact of the identified faults in terms of CO₂ emissions and operating costs to support the development of data-driven AFDD tools. Section 2 describes the experimental set-up, while Section 3 details the experimental tests. Section 4 compares the boundary conditions of the experiments, while Section 5 discusses the effects associated with the faults' occurrence.

2. EXPERIMENTAL SET-UP

The SENS i-Lab is an innovative, multi-sensorial and multi-purpose laboratory of the Department of Architecture and Industrial Design of the University of Campania Luigi Vanvitelli (Aversa, south of Italy) [21]. It mainly consists of an integrated test room served by a typical HVAC system, including a single-duct dual-fan constant air volume AHU, able to control indoor air temperature, indoor air relative humidity, indoor air velocity and indoor air quality. Figure 1

reports the schematic configuration of the AHU that is fully equipped in order to monitor, control and record the key parameters of the system. Among the other components, the AHU includes three dampers (exhaust air damper D_{EA} , outdoor air damper D_{OA} and return air damper D_{RA}). All of them are manufactured by the CLA s.r.l. company [22]. Each damper is characterized by a frame in galvanised steel (thickness of 1.0 mm) and airfoil blades are in galvanised steel (with thickness of 0.5+0.5 mm and distance between blades of 100 mm). They are categorized as Class 4 according to EN 1751 Standard [23]. The dimensions of D_{EA} , D_{OA} and D_{RA} , respectively, are the following: 70×41 cm², 70×31 cm² and 40×11 cm². The AHU is also equipped with three filters (return air filter RAFil, outdoor air filter OAFil, and supply air filter SAFil). All the filters are manufactured by the F.C.R. company [24], with the following sizes (long side, short side, and thickness): 59.2×28.7×4.8 cm³ for RAFil, 59.2×28.7×9.8 cm³ for OAFil, and 59.2×28.7×28.2 cm³ for SAFil. RAFil and OAFil are identical. Filter media is a progressive density synthetic fibre. Both filters are classified as ISO Coarse class 50% according to ISO 16890 [25]. The outdoor air filter is characterized by a nominal airflow rate of 2300 m³/h across a 0.4 m² filtering area, with a pressure drop of 70 Pa. In contrast, the return air filter has a nominal airflow rate of 1650 m³/h over a 0.3 m² filtering area, with a pressure drop of 70 Pa. SAFil is a 3V rigid bag filter with injection-moulded plastic (polystyrene) frame. Its filtering medium is a water repellent fiberglass paper pleated at calibrated pitch with continuous thermoplastic wire separation. It is classified as ePM1 85% according to ISO 16890 [25]. This filter is characterized by a nominal pressure drop of 110 Pa at a nominal airflow rate of 1700 m³/h.

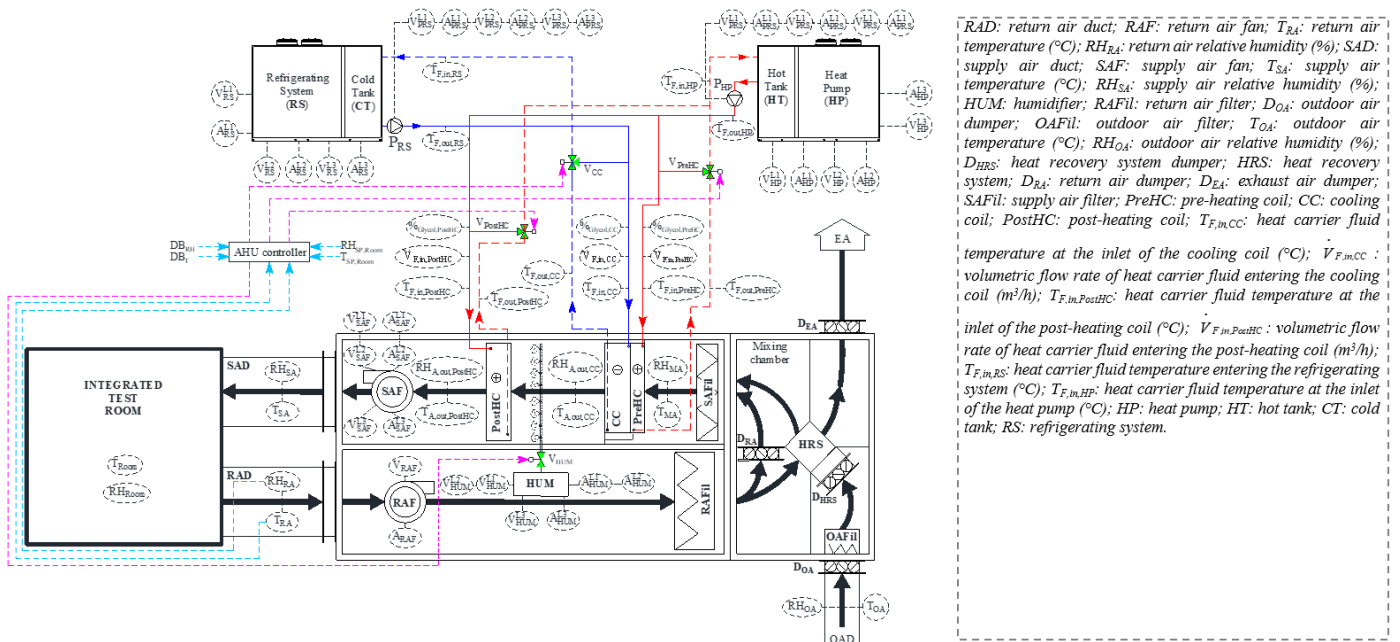


Figure 1. Schematic of the AHU of the SENS i-Lab

The AHU is operated according to a specific control logic. In particular, the following parameters are manually set (and eventually modified during the tests) by the end-users: (i) the desired room setpoint of both indoor air temperature ($T_{SP,Room}$) and indoor air relative humidity ($RH_{SP,Room}$); (ii) the $T_{SP,Room}$ deadband DB_T and $RH_{SP,Room}$ deadband DB_{RH} ; (iii) the return

air fan (OL_{RAF}) and the supply air fan (OL_{SAF}) velocity; (iv) the return air damper opening percentage (OP_{DRA}), the outdoor air damper (OP_{DOA}) opening percentage, the exhaust air damper opening percentage (OP_{DEA}); (v) the activation of the static heat-recovery system damper (OP_{DHRS}). The parameters OP_{DRA} , OP_{DOA} and OP_{DEA} can range between 0 and 100%,

where 100% means that the damper is fully open and 0% fully closed. The parameter OP_{DHRs} can be set to 100% (the heat recovery does not occur) or 0% (the heat recovery from return air flow takes place). Once the previous parameters are manually set by the end-users, the opening percentages of the valves supplying the pre-heating coil (OP_{V_PreHC}), the post-heating coil (OP_{V_PostHC}), the cooling coil (OP_{V_CC}) and the humidifier (OP_{V_HUM}) are automatically managed between 0 and 100% by PID (proportional-integral-derivative) controllers in order to maintain the desired room setpoint. Alternatively, at the beginning or during the test, the end-users can also manually force the opening percentages of the valves (OP_{V_PreHC} , OP_{V_PostHC} , OP_{V_CC} and OP_{V_HUM}) for research purposes. Even if the AHU is equipped with a pre-heating coil and a heat recovery system, these components have been always manually deactivated during the tests. Additional details about the characteristics of the AHU can be found in [10, 11].

3. EXPERIMENTAL TESTS

Twenty-eight daily fault free and faulty experiments are carried out (from 9:00 a.m. up to 6:00 p.m.) in order to investigate the AHU behaviour under Italian summer and winter seasons. In particular, 14 tests (SN1, SN2, SN3, SN4, SN5, SN6, SN7, WN1, WN2, WN3, WN4, WN5, WN6 and WN7) have been performed under normal (N) conditions; in more detail, the tests (SN1, SN2, SN3, SN4, SN5, SN6 and SN7) have been carried out during the summer 2022 (S), while the other tests (WN1, WN2, WN3, WN4, WN5, WN6 and WN7) have been developed during the winter 2022/23 (W). The remaining 14 experiments (SF1, SF2, SF3, SF4, SF5, SF6, SF7, WF1, WF2, WF3, WF4, WF5, WF6, and WF7) have been performed during both the summer 2022 (S) and the winter 2023 (W) while manually forcing the positions of the dampers or partially clogging filters (by covering the filters with a single-wall corrugated cardboard, where the covered area (CP) represented the fault severity). Table 1 reports the operating conditions associated to the faulty experiments in terms of opening percentages of the return air damper (OP_{DRA}), the outdoor air damper (OP_{DOA}) and the exhaust air damper (OP_{DEA}), as well as the CP of the return air filter, the outdoor air filter and the supply air filter (CP_{RAFil} , CP_{OAFil} and CP_{SAFil} , respectively).

Table 1. Operating conditions of the faulty experiments

ID Test	OP_{DRA} (%)	OP_{DOA} (%)	OP_{DEA} (%)	CP_{RAFil} (%)	CP_{OAFil} (%)	CP_{SAFil} (%)
SF1	0	20	20	0	0	0
SF2	100	0	20	0	0	0
SF3	100	100	20	0	0	0
SF4	100	20	0	0	0	0
SF5	100	20	0	0	50	0
SF6	100	20	0	0	0	50
SF7	100	20	0	50	0	0
WF1	0	20	20	0	0	0
WF2	100	0	20	0	0	0
WF3	100	100	20	0	0	0
WF4	100	20	0	0	0	0
WF5	100	20	0	0	50	0
WF6	100	20	0	0	0	50
WF7	100	20	0	50	0	0

All tests, conducted under both normal and faulty

conditions, were performed with TSP,Room and RHSP,Room set to 26°C (with a DBT of 1°C) and 50% (with a DBRH of 5%), respectively, during summer. Conversely, during winter, TSP,Room and RHSP,Room were set to 20°C (with a DBT of 1°C) and 50% (with a DBRH of 5%). The supply and return air fan velocities were maintained at 50%, regardless of the test conditions.

4. COMPARISON OF BOUNDARY CONDITIONS DURING FAULT FREE AND FAULTY TESTS

To highlight the impact of the faults under investigation, the tests conducted under normal conditions (SN1-SN7 and WN1-WN7) have been adopted as baselines to be compared with the tests carried out under faulty conditions (SF1-SF7 and WF1-WF7). All normal and faulty tests are characterized by the same starting time (which is 9 a.m.) as well as the same initial return air temperature $T_{RA,initial}$ (equal to approximately 28°C for summer tests and 18°C for winter tests), and the same initial return air relative humidity $RH_{RA,initial}$ (approximately equal to 60% for both summer and winter tests). The average absolute difference between normal and faulty tests in terms of outdoor air temperature T_{OA} and outdoor air relative humidity RH_{OA} has been calculated and they have been assumed as comparable in the case of such difference is lower than 1.5°C for T_{OA} and 10% for RH_{OA} . According to these criteria, the following pairs of tests can be assumed as comparable and, therefore, be used to determine the effects of each fault on the behaviour of the AHU: SN1 vs. SF2, SN2 vs. SF5, SN3 vs. SF1, SN4 vs. SF4, SN5 vs. SF3, SN5 vs. SF6, SN6 vs. SF7, WN1 vs. WF1, WN1 vs. SF3, WN3 vs. WF2, WN2 vs. WF7, WN3 vs. WF2, WN4 vs. WF6, WN5 vs. WF4. More details about the above-described methodology can be found in references [10, 11].

5. ASSESSMENT OF FAULTS' SYMPTOMS IN TERMS OF COMFORT, ELECTRIC ENERGY DEMAND, CO₂ EMISSIONS AND OPERATING COSTS

In this section, the comparison between the fault free tests and the corresponding faulty tests has been performed, from different points of view, to highlight the impact of each investigated fault on the AHU performance. In particular, the Section 5.1 summarizes the effects of the selected faults on both comfort and electric energy demand; the Section 5.2 focuses on global equivalent CO₂ emissions, while the Section 5.3 shows the impacts on operating costs.

5.1 Effects of fault on comfort and electric energy demand

The above-mentioned normal and faulty tests have been compared in terms of comfort and electric energy demands. In particular, Figure 2 reports the percentage comfort time difference (%DCT) between each faulty and corresponding normal calculated as follows:

$$\% \Delta CT = CT_{Faulty} - CT_{Normal} \quad (1)$$

where, CT_{Faulty} and CT_{Normal} represent the percentage of time under thermal or hygrometric comfort conditions (i.e., the percentage of time during which indoor air temperature or relative humidity is within the given deadbands)

corresponding to faulty and normal tests, respectively. A negative value of this parameter indicates that the hours of comfort associated with the faulty test are lower than the corresponding normal test.

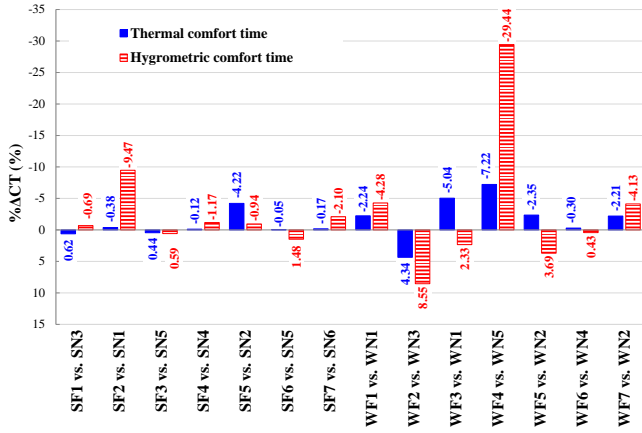


Figure 2. Values of %DCT as a function of the tests

The comparison in terms of %DCT highlights that the worst fault in terms of hygrometric comfort time is the fault F4 (exhaust air damper stuck at 0%) during winter, which corresponds to a considerable reduction by about 29% with respect to the test WN5.

Figure 3 reports the parameter %DEE indicating the percentage difference between the faulty and the corresponding normal test in terms of daily electric consumption:

$$\% \Delta EE = \frac{(EE_{Faulty} - EE_{Normal})}{EE_{Normal}} \times 100 \quad (2)$$

where, EE_{Faulty} and EE_{Normal} are, respectively, the electric energy consumption of AHU during the faulty test and the corresponding normal test. A positive value of this parameter means that the electric energy demand associated with the faulty test is larger than the corresponding normal test.

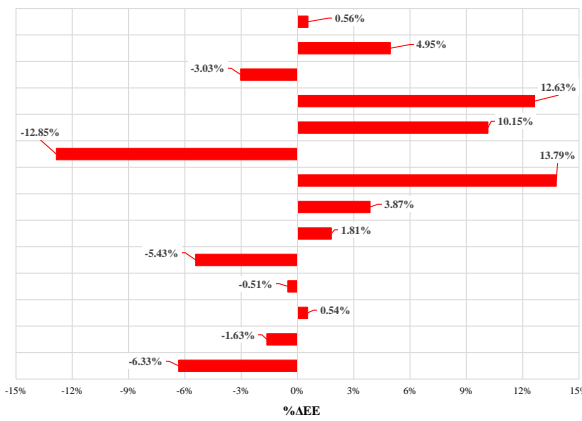


Figure 3. Values of %DEE as a function of the tests

This figure underlines that the occurrence of the faults is not really relevant during summer, with values of %DEE ranging between -6.33% and +3.87%; in particular, the most adverse fault during summer in terms of %DEE is F7. Conversely, the faults are characterized by a significant impact in terms of electric demand during winter; in more detail, the faults F1,

F3, and F4 cause a greater consumption in comparison to the normal operation by 13.79%, 10.15%, and 12.63%, respectively.

5.2 Effects of faults on global equivalent CO₂ emissions

The environmental assessment is performed through an energy output-based emission factor approach [26]. According to this approach, the mass m_x of a given pollutant x emitted while producing the energy output EE , can be worked out as:

$$m_x = u_x^{EE} \times EE \quad (3)$$

where, u_x^{EE} is the energy output-based emission factor, that is the specific emissions of x per unit of EE . This factor depends upon several operating and structural variables, such as the specific equipment, partial load operation, age, state of maintenance, outdoor conditions, and pollutant abatement systems. CO₂ emissions prove to be quantitatively much more important than other greenhouse gas emissions [27]. In particular, the CO₂ emission factor associated to the electricity generation in Italy $u_{CO_2}^{EE}$ depends on day as well as the time of the day. Figure 4 reports this factor for each couple of corresponding normal and faulty tests as a function of the time derived from the study [28] according to the day during which the faulty test has been performed (by assuming that each faulty test and its corresponding normal test take place on the same day).

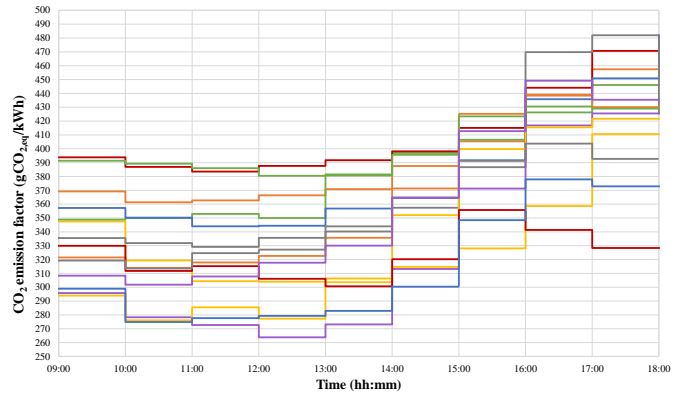


Figure 4. CO₂ emission factor associated to electricity consumption as a function of both tests and time [28]

The AHU environmental performance associated to the faulty tests in comparison with those of the corresponding normal tests have been assessed as follows:

$$\% \Delta m_{CO_2} = \frac{(m_{CO_2, Faulty} - m_{CO_2, Normal})}{m_{CO_2, Normal}} \times 100 \quad (4)$$

$$= \frac{(u_{CO_2}^{EE} \times EE_{Faulty} - u_{CO_2}^{EE} \times EE_{Normal})}{u_{CO_2}^{EE} \times EE_{Normal}} \times 100$$

where, $m_{CO_2, Faulty}$ and $m_{CO_2, Normal}$ are, respectively, the global equivalent CO₂ emissions of AHU components in the case of faulty and normal conditions, EE_{Faulty} and EE_{Normal} are the electric energy consumptions during faulty tests and corresponding normal tests, respectively. A positive value of

this parameter indicates that the global equivalent CO₂ emissions associated with the faulty test are larger than those corresponding to the normal test.

Figures 5 and 6 indicate the parameter % Δm_{CO_2} as a function of the tests, with instantaneous values calculated time-step by time-step and reported in descending order, for the summer and winter tests, respectively.

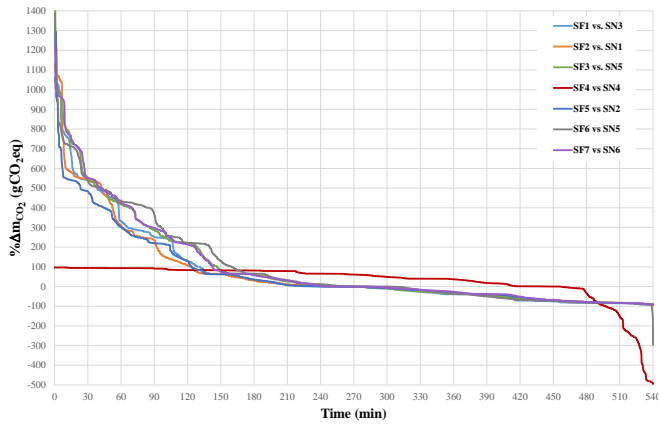


Figure 5. % Δm_{CO_2} calculated time-step by time-step in descending order as a function of the summer tests

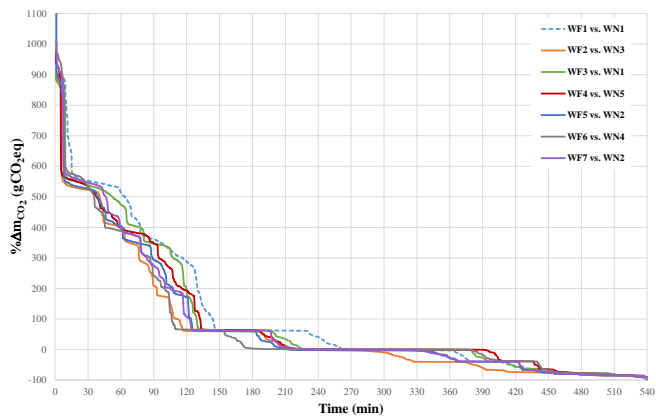


Figure 6. % Δm_{CO_2} calculated time-step by time-step in descending order as a function of the winter tests

Specifically, with reference to the summer tests (Figure 5), positive values of % Δm_{CO_2} are observed during a period of about 240 minutes (corresponding to 40% of the entire tests' durations), whatever the couple of tests under investigation is (except the case of SF4 vs. SN4); values of % Δm_{CO_2} close to zero can be recognized for about 40 minutes, while the remaining parts correspond to negative values of % Δm_{CO_2} . The maximum value of % Δm_{CO_2} is about 1358%, while the minimum corresponds to a value of about -493%; the average value is equal to about 75% considering all the summer tests. With reference to the winter tests (Figure 6), positive values of % Δm_{CO_2} are recognized during a period of about 210 minutes (corresponding to 30% of the entire tests' durations), whatever the couple of tests under investigation is; values of % Δm_{CO_2} close to zero are obtained for about 20 minutes, while negative values of % Δm_{CO_2} correspond to the remaining parts of the tests. The maximum value of % Δm_{CO_2} is about 1302%, while the minimum corresponds to a value of about -90%; the average is equal to about 85% considering all the winter tests.

Table 2 reports the daily values of % Δm_{CO_2} as a function of the tests.

Table 2. Daily values of % Δm_{CO_2} as a function of the tests

Tests under Comparison	% Δm_{CO_2}
SF1 vs. SN3	-6.19%
SF2 vs. SN1	-1.81%
SF3 vs. SN5	0.51%
SF4 vs. SN4	110.15%
SF5 vs. SN2	-5.51%
SF6 vs. SN5	2.26%
SF7 vs. SN6	3.80%
WF1 vs. WN1	13.65%
WF2 vs. WN3	-12.41%
WF3 vs. WN1	9.95%
WF4 vs. WN5	12.95%
WF5 vs. WN2	-3.08%
WF6 vs. WN4	4.54%
WF7 vs. WN2	1.18%

The values in this table indicate that: (i) the fault 4 (i.e., exhaust air dumper kept always closed) is characterized by a relevant effect under both summer and winter conditions, with daily values of % Δm_{CO_2} corresponding to about 110% and 13%, respectively; the fault 1 (i.e., return air damper kept always closed) significantly impacts the CO₂ emissions during winter only, with a notable daily increment by about 14% in comparison to the normal case. The faults 2 and 5 correspond to negative daily values of % Δm_{CO_2} during both summer and winter; this means that they reduce the global equivalent CO₂ emissions with respect to the fault free tests, whatever the season is. However, the reduced environmental impact (due to a reduced electric energy consumption, as indicated in Figure 3) is compensated by a lower daily thermal/hygrometric comfort time during the summer period in the cases of both the faults 2 and 5 and during the winter period for the fault 5 only. The results associated to the occurrence of the fault 2 during winter can be explained by taking into account that the absence of outdoor air allows smaller fluctuations of indoor air humidity as well as more stable hygrometric conditions in addition, it can be noticed that a relevant reduction of humidifier operation time during the winter faulty test can be recognized with respect to the corresponding normal test. In the case of the fault 1, Table 2 indicates that, with respect to the normal test, the faulty operation is characterized by lower daily global equivalent CO₂ emissions during summer only, together with reduced electric energy demand (Figure 3) and negligible variations in terms of thermo/hygrometric comfort time; this result is because the utilization of hot outdoor air is more than counterbalanced by the significantly decreased supply airflow rate elaborated by the AHU.

5.3 Effects of faults on operating costs

In this paper, the operating costs associated to the electric energy consumption are evaluated. Figure 7 reports the unit cost of electricity for each couple of faulty and normal tests according to the Italian scenario [29]. Similar to the environmental analysis, no difference in terms of unit cost is assumed between the faulty test and the associated normal test.

The operating costs of AHU associated with the occurrence of the faults are compared with those corresponding to the fault free tests by using the following formula:

$$\begin{aligned} \% \Delta OC &= \frac{(OC_{Faulty} - OC_{Normal})}{OC_{Normal}} \times 100 \\ &= \frac{(UC_{EE} \times EE_{Faulty} - UC_{EE} \times EE_{Normal})}{UC_{EE} \times EE_{Normal}} \times 100 \end{aligned} \quad (5)$$

where, OC_{Faulty} and OC_{Normal} are, respectively, the operating costs of AHU under faulty and normal conditions, EE_{Faulty} and EE_{Normal} are the electric energy consumptions during faulty and normal tests, respectively, and UC_{EE} is the unit cost of electricity purchased from the grid according to the values in Figure 7. A positive value of %DOC indicates that the operating costs associated with the faulty test are larger than those of the corresponding normal test.

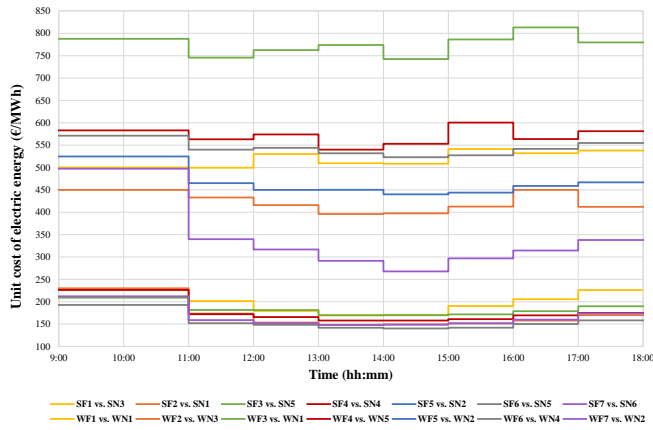


Figure 7. Unit cost of electricity purchased from the grid as a function of both the tests and the time [29]

Figures 8 and 9 show the parameter %DOC as a function of the tests, with values calculated time-step by time-step and reported in descending order, for the summer and winter tests, respectively. Specifically, with reference to the summer tests (Figure 8), positive values are observed during a period of about 250 minutes (corresponding to 45% of the entire tests' durations), whatever the couple of tests under investigation is (except the case of SF4 vs. SN4); values of %DOC close to zero can be recognized for about 40 minutes, while the remaining parts correspond to negative values of %DOC. The maximum value of %DOC is about 3094%, while the minimum corresponds to a value of about -83% as well as the average is equal to about 133%. With reference to the winter tests (Figure 9), positive values of %DOC are recognized during a period of about 230 minutes (corresponding to 35% of the entire tests' durations), whatever the couple of tests under investigation are; values of %DOC close to zero are obtained for about 130 minutes, while negative values of %DOC correspond to the remaining parts of the tests. The maximum value of %DOC is about 1302%, while the minimum corresponds to a value of about -90% as well as the average is equal to about 85%.

Table 3 indicates the daily values of %DOC as a function of the tests. The values in this table indicate that: (i) the fault 4 (i.e., exhaust air damper kept always closed) is characterized by a relevant effect under both summer and winter conditions, with daily values of %DOC corresponding to 110% and 12%, respectively; the fault 1 (i.e., return air damper kept always closed) and the fault 3 (i.e., fresh air damper kept always open) significantly impact the daily operating costs during winter only, with notable daily increments by about 13% and 10%, respectively, in comparison to the normal cases.

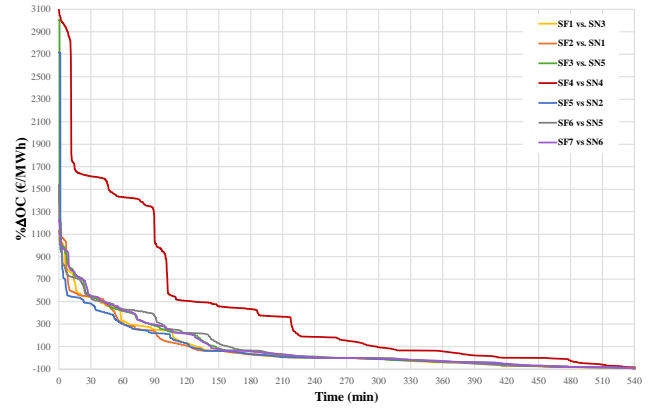


Figure 8. Values of %DOC calculated time-step by time-step in descending order as a function of the summer tests

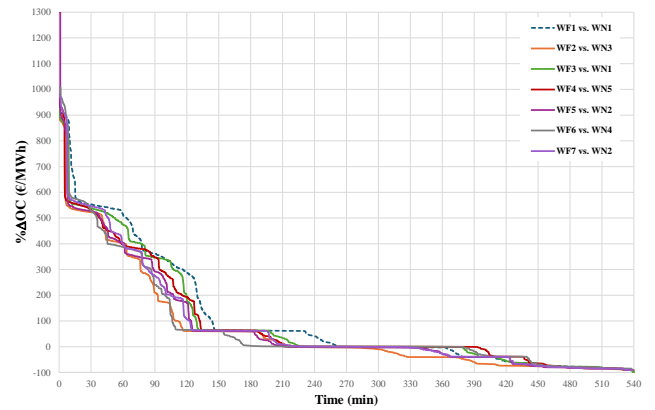


Figure 9. Values of %DOC calculated time-step by time-step in descending order as a function of the winter tests

Table 3. Daily values of %DOC as a function of the tests

Tests under Comparison	%ΔOC
SF1 vs. SN3	-19.16%
SF2 vs. SN1	-1.47%
SF3 vs. SN5	0.64%
SF4 vs. SN4	110.44%
SF5 vs. SN2	-5.28%
SF6 vs. SN5	1.87%
SF7 vs. SN6	4.01%
WF1 vs. WN1	13.17%
WF2 vs. WN3	-12.76%
WF3 vs. WN1	10.14%
WF4 vs. WN5	11.99%
WF5 vs. WN2	-3.28%
WF6 vs. WN4	5.46%
WF7 vs. WN2	0.50%

The faults 2 and 5 correspond to negative daily values of %DOC during both summer and winter; this means that they reduce the operating costs with respect to the fault free tests, whatever the season is. However, the reduced economic impact (due to a reduced electric energy demand, as indicated in Figure 3) is balanced by a lower thermal/hygrometric comfort time during the summer period in the cases of both the faults 2 and 5 and during the winter period for the fault 5 only. The results associated with the occurrence of the fault 2 during winter can be explained by taking into account the absence of outdoor air causes reduced fluctuations in terms of indoor air

humidity as well as more stable hygrometric conditions; in addition, it can be noticed that a relevant reduction of humidifier operation time during the winter faulty test can be recognized with respect to the corresponding normal test. In the case of the fault 1, Table 3 indicates that, with respect to the normal test, the faulty operation is characterized by lower operating costs during summer only, together with reduced electric energy demand (Figure 3) and negligible variations in terms of thermo/hygrometric comfort; this is due to the fact that the utilization of hot outdoor air is more than counterbalanced by the significantly decreased supply airflow rate elaborated by the AHU.

6. CONCLUSIONS

The effects of 7 typical faults on the performance of a typical AHU have been investigated in terms of thermo-hygrometric comfort time, electric energy demand, global equivalent CO₂ emissions, and operating costs. The assessment has been performed by contrasting experimental data associated with fault-free and faulty tests carried out under similar boundary conditions, during both summer and winter of southern Italy. The results indicated that the fault corresponding to the exhaust air dumper kept always closed is the most adverse one, with relevant effects under both summer and winter conditions. In particular, it enhances the daily global equivalent CO₂ emissions by about 110% and 13%, respectively, during summer and winter with respect to normal operation. In addition, it increases the daily operating costs by about 110% and 12%, respectively, in comparison to the fault-free conditions.

In the future, the authors would like to perform additional investigations with the aim of extending the analysis on different faults in order to develop and validate an innovative data-driven algorithm customized to the experimental results for performing automated fault detections and diagnoses on typical AHUs.

ACKNOWLEDGMENT

This study has been performed within the activities of the research project titled “UTMOST FDD: an aUToMated, Open, Scalable and Transparent Fault Detection and Diagnosis process for air-handling units based on a hybrid expert and artificial intelligence approach. From experimental open data to transfer model learning for the enhancement of energy management and indoor environmental quality in buildings” funded by the call “PRIN 22” (CUP: E53D23002840006).

REFERENCES

[1] UNEP. (2022). 2022 global status report for buildings and construction. <https://www.unep.org/resources/publication/2022-global-status-report-buildings-and-construction>.

[2] Yun, W.S., Hong, W.H., Seo, H. (2021). A data-driven fault detection and diagnosis scheme for air handling units in building HVAC systems considering undefined states. *Journal of Building Engineering*, 35: 102111. <https://doi.org/10.1016/j.jobee.2020.102111>

[3] Wang, H., Chen, Y. (2016). A robust fault detection and

diagnosis strategy for multiple faults of VAV air handling units. *Energy and Buildings*, 127: 442-451. <https://doi.org/10.1016/j.enbuild.2016.06.013>

[4] Deshmukh, S., Samouhos, S., Glicksman, L., Norford, L. (2019). Fault detection in commercial building VAV AHU: A case study of an academic building. *Energy and Buildings*, 201: 163-173. <https://doi.org/10.1016/j.enbuild.2019.06.051>

[5] D’Urso, D., Sinatra, A., Compagno, L., Chiacchio, F. (2022). Assessment of the optimal preventive maintenance period using stochastic hybrid modelling. *Procedia Computer Science*, 200: 1664-1673. <https://doi.org/10.1016/j.procs.2022.01.367>

[6] Sanzana, M.R., Maul, T., Wong, J.Y., Abdulrazic, M. O.M., Yip, C.C. (2022). Application of deep learning in facility management and maintenance for heating, ventilation, and air conditioning. *Automation in Construction*, 141: 104445. <https://doi.org/10.1016/j.autcon.2022.104445>

[7] Mirnaghi, M.S., Haghghat, F. (2020). Fault detection and diagnosis of large-scale HVAC systems in buildings using data-driven methods: A comprehensive review. *Energy and Buildings*, 229: 110492. <https://doi.org/10.1016/j.enbuild.2020.110492>

[8] Yu, Y., Woradechjumroen, D., Yu, D. (2014). A review of fault detection and diagnosis methodologies on air-handling units. *Energy and Buildings*, 82: 550-562. <https://doi.org/10.1016/j.enbuild.2014.06.042>

[9] Dexter, A., Pakanen, J. (2024). Demonstrating automated faults detection and diagnosis methods in real buildings. *IEA ECBCS annex 34 Handbook*.

[10] Rosato, A., Guarino, F., El Youssef, M., Capozzoli, A., Masullo, M., Maffei, L. (2022). Experimental assessment of ground-truth faults in a typical single-duct dual-fan air-handling unit under Mediterranean climatic conditions: Impact scenarios of sensors’ offset and fans’ failure. *Energy and Buildings*, 275: 112492. <https://doi.org/10.1016/j.enbuild.2022.112492>

[11] Rosato, A., Guarino, F., El Youssef, M., Capozzoli, A., Masullo, M., Maffei, L. (2022). Faulty operation of coils’ and humidifier valves in a typical air-handling unit: Experimental impact assessment of indoor comfort and patterns of operating parameters under mediterranean climatic conditions. *Energies*, 15(18): 6781. <https://doi.org/10.3390/en15186781>

[12] Frank, S., Lin, G., Jin, X., Singla, R., Farthing, A., Granderson, J. (2019). A performance evaluation framework for building fault detection and diagnosis algorithms. *Energy and Buildings*, 192: 84-92. <https://doi.org/10.1016/j.enbuild.2019.03.024>

[13] Piscitelli, M.S., Mazzarelli, D.M., Capozzoli, A. (2020). Enhancing operational performance of AHUs through an advanced fault detection and diagnosis process based on temporal association and decision rules. *Energy and Buildings*, 226: 110369. <https://doi.org/10.1016/j.enbuild.2020.110369>

[14] Wen, J., Li, S. (2012). ACCURIS. RP-1312-Tools for Evaluating Fault Detection and Diagnostic Methods for Air-Handling Units. Atlanta, Georgia, USA. https://store.accuristech.com/standards/rp-1312-tools-for-evaluating-fault-detection-and-diagnostic-methods-for-air-handling-units?product_id=1833299.

[15] Lin, G., Kramer, H., Granderson, J. (2020). Building fault detection and diagnostics: Achieved savings, and

methods to evaluate algorithm performance. *Building and Environment*, 168: 106505. <https://doi.org/10.1016/j.buildenv.2019.106505>

[16] Rosato, A., Mercuri, R., Guarino, F., El Youssef, M. (2024). Faults' effects in air-handling units: A comprehensive analysis of numerical studies. In *Sustainability in Energy and Buildings 2023*, pp. 613-625. https://doi.org/10.1007/978-981-99-8501-2_53

[17] Granderson, J., Lin, G., Harding, A., Im, P., Chen, Y. (2020). Building fault detection data to aid diagnostic algorithm creation and performance testing. *Scientific Data*, 7(1): 65. <https://doi.org/10.1038/s41597-020-0398-6>

[18] Carling, P. (2002). Comparison of three fault detection methods based on field data of an air-handling unit. *ASHRAE Transactions*, 108: 904-921.

[19] Nehasil, O., Dobiášová, L., Mazanec, V., Široký, J. (2021). Versatile AHU fault detection—Design, field validation and practical application. *Energy and Buildings*, 237: 110781. <https://doi.org/10.1016/j.enbuild.2021.110781>

[20] Rosato, A., El Youssef, M., Guarino, F., Ciervo, A., Sibilio, S. (2022). Experimental studies of air-handling units' faulty operation for the development of data-driven fault detection and diagnosis tools: A systematic review. *Energy Reports*, 8: 494-503. <https://doi.org/10.1016/j.egy.2022.10.087>

[21] Masullo, M. (2020). SENS i-La. [https://www.architettura.unicampania.it/images/ricerca/aboratori/EN/SENS-i_Lab_2021_EN.pdf](https://www.architettura.unicampania.it/images/ricerca/laboratori/EN/SENS-i_Lab_2021_EN.pdf).

[22] CLA. DLT101Z. <https://www.cla.it/en/products/adjustment/dlt101z/>.

[23] UNI EN 1751:2014. (2014). Ventilation for buildings—Air terminal devices—Aerodynamic testing of damper and valves. <https://store.uni.com/en/uni-en-1751-2014>.

[24] F.C.R. Filtrazione Condizionamento Riscaldamento S.p.A. <https://fcr.it/?lang=en4>.

[25] ISO 16890-1:2016. (2016). Air filters for general ventilation—Part 1: Technical specifications, requirements, and classification system based upon particulate matter efficiency (ePM). <https://www.iso.org/standard/57864.html>.

[26] Chicco, G., Mancarella, P. (2008). Assessment of the greenhouse gas emissions from cogeneration and trigeneration systems. Part I: Models and indicators. *Energy*, 33(3): 410-417. <https://doi.org/10.1016/j.energy.2007.10.006>

[27] Harvey, L.D. (2012). *A Handbook on Low-Energy Buildings and District-Energy Systems: Fundamentals, Techniques and Examples*. Routledge.

[28] Electricity Maps. <https://www.electricitymaps.com>.

[29] GME. <https://www.mercatoelettrico.org/it/>.

NOMENCLATURE

AFDD	Automatic fault detection and diagnosis
AHU	Air-Handling Unit
CO ₂	Carbon dioxide
CP	Clogging percentage, %
CT	Comfort time, %
D _{EA}	Exhaust air damper
D _{HRS}	Heat-recovery system damper
D _{OA}	Outdoor air damper
D _{RA}	Return air damper
DB	Deadband
EE	Electric energy, kWh
HVAC	Heating, ventilation and air-conditioning
m_{CO_2}	Mass of global equivalent CO ₂ emissions, kg
OAFil	Outdoor air filter
OC	Operating costs, €
OL	Fan velocity percentage, %
OP	Opening percentage, %
RAFil	Return air filter
RH	Relative humidity, %
SAFil	Supply air filter
SF1-SF7	Faulty tests during summer
SN1-SN6	Normal tests during summer
T	Temperature, °C
UC	Unit cost, €/kWh
$u_{CO_2}^{EE}$	CO ₂ emission factor associated with electric energy consumption, kg/MWh
WF1-WF7	Faulty tests performed during winter
WN1-WN5	Normal tests performed during winter

Greek symbols

D	Difference, %
---	---------------

Subscripts

Faulty	Faulty test
Normal	Normal test
OA	Outdoor air
RA	Return air
RAF	Return air fan
SAF	Supply air fan
V _{CC}	Cooling coil valve
V _{HUM}	Humidifier valve
V _{PostHC}	PostHC valve